Catalytic Mechanism of Nucleoside Diphosphate Kinase Investigated Using Nucleotide Analogues, Viscosity Effects, and X-ray Crystallography[†,‡]

Philippe Gonin,[§] Yingwu Xu,[||] Laurence Milon,[⊥] Sandrine Dabernat,[@] Michael Morr,[$] Rakesh Kumar,[&] Marie-Lise Lacombe,[⊥] Joël Janin,[||] and Ioan Lascu*[,§]

University of Bordeaux-2, Institut de Biochimie et Génétique Cellulaires, UPR 9026, Centre National de la Recherche Scientifique, 33077 Bordeaux, France, Laboratoire d'Enzymologie et Biochimie Structurales, UPR 9063, Centre National de la Recherche Scientifique, 91198 Gif-sur-Yvette, France, Unité INSERM 402, 75571 Paris, France, Laboratoire de Biologie Cellulaire, University of Bordeaux-2, 33077 Bordeaux, France, Gesellschaft für Biotechnologische Forschung mbH, D-38124 Braunschweig, Germany, and Faculty of Medicine, University of Alberta, Edmonton, Alberta, Canada T6G 2H7

Received December 18, 1998; Revised Manuscript Received March 29, 1999

ABSTRACT: Nucleoside diphosphate (NDP) kinases display low specificity with respect to the base moiety of the nucleotides and to the 2′-position of the ribose, but the 3′-hydroxyl is found to be important for catalysis. We report in this paper the enzymatic analysis of a series of derivatives of thymidine diphosphate (TDP) where the 3′-OH group was removed or replaced by fluorine, azido, and amino groups. With *Dictyostelium* NDP kinase, k_{cat} decreases 15−200-fold from 1100 s^{-1} with TDP, and $(k_{cat}/K_m)_{NDP}$ decreases from 12×10^6 to 10^3 to 5×10^4 M^{-1} s^{-1}, depending on the substrate. The poorest substrates are 3′-deoxyTDP and 3′-azido-3′-deoxyTDP, while the best modified substrates are 2′,3′-dehydro-3′-deoxyTDP and 3′-fluoro-3′-deoxyTDP. In a similar way, 3′-fluoro-2′,3′-dideoxyUDP was found to be a better substrate than 2′,3′-dideoxyUDP, but a much poorer substrate than 2′-deoxyUDP. $(k_{cat}/K_m)_{NDP}$ is sensitive to the viscosity of the solution with TDP as the substrate but not with the modified substrates. To understand the poor catalytic efficiency of the modified nucleotides at a structural level, we determined the crystal structure of *Dictyostelium* NDP kinase complexed to 3′-fluoro-2′,3′-dideoxyUDP at 2.7 Å resolution. Significant differences are noted as compared to the TDP complex. Substrate-assisted catalysis by the 3′-OH, which is effective in the NDP kinase reaction, cannot occur with the modified substrate. With TDP, the β-phosphate, which is the leaving group when a γ-phosphate is transferred to His122, hydrogen bonds to the 3′-hydroxyl group of the sugar; with 3′-fluoro-2′,3′-dideoxyUDP, the β-phosphate hydrogen bonds to Asn119 and moves away from the attacking Nδ of the catalytic His122. Since all anti-AIDS nucleoside drugs are modified at the 3′-position, these results are relevant to the role of NDP kinase in their cellular metabolism.

The nucleoside diphosphate (NDP)[1] kinases catalyze the reversible phosphorylation of nucleoside diphosphates by nucleoside triphosphates, via a covalent intermediate (*1*, *2*). The active-site histidine is transiently phosphorylated at the Nδ position (*3*−*5*).

$$N_1TP + E{-}His \leftrightarrow N_1DP + E{-}His{-}P \quad (1a)$$

$$N_2DP + E{-}His{-}P \leftrightarrow N_2TP + E{-}His \quad (1b)$$

$$N_1TP + N_2DP \leftrightarrow N_1DP + N_2TP \quad (1)$$

Several crystal structures have been obtained, of free NDP kinase (*6*−*8*), of the phosphorylated intermediate (*4*), of the enzyme complexed with ADP (*9*, *10*), GDP (*11*), TDP (*12*), and AZT-DP (*13*), and of the enzyme complexed with ADP and AlF_3, a putative transition state analogue (*14*). The contacts between the nucleotides and the protein are well-defined and remarkably conserved in enzymes from different sources from bacteria to humans. The base moiety lies in a hydrophobic crevice and makes no specific polar interactions with the protein. The 2′-OH is not required for binding or catalysis. This fits well with the broad specificity of all NDP kinases, needed for the in vivo function.

A unique feature is the compact conformation of the enzyme-bound nucleotides. The 3′-OH is within hydrogen-bonding distance of the oxygen bridging the β- and γ-phosphates of the NTP substrate. Rapid mixing studies (*15*) and steady state experiments (*16*, *17*) showed that the absence

[†] This work was supported by grants from Agence Nationale de la Recherche contre le SIDA, Association pour la Recherche sur le Cancer, the Fondation pour la Recherche Médicale, and the Conseil Régional d'Aquitaine. Part of this work was supported by an Establishment Grant and Scholar Award from the Alberta Heritage Foundation for Medical Research, Edmonton, AB (to R.K.).

[‡] The coordinates have been deposited with the Protein Data Bank (file name 1b99).

* To whom corrspondence should be addressed: University of Bordeaux-2, IBGC-CNRS, 1 rue Camille Saint-Saëns, 33077 Bordeaux, France. Telephone and fax: (33) 5 56 99 90 11. E-mail: ioan.lascu@ibgc.u-bordeaux2.fr.

[§] UPR 9026, Centre National de la Recherche Scientifique.

[||] UPR 9063, Centre National de la Recherche Scientifique.

[⊥] Unité INSERM 402.

[@] University of Bordeaux-2.

[$] Gesellschaft für Biotechnologische Forschung mbH.

[&] University of Alberta.

[1] Abbreviations: NDP, nucleoside diphosphate; NTP, nucleoside triphosphate; AZT, 3′-azido-3′-deoxythymidine; PEG, polyethylene glycol.

10.1021/bi982990v CCC: $18.00
Published on Web 05/13/1999

of the ribose 3′-OH dramatically decreases the catalytic efficiency of the enzyme. This is important, for all nucleoside analogues used in anti-AIDS therapy lack this hydroxyl group (*18*). After being converted to triphosphates by cellular kinases, they become substrates of the viral reverse transcriptase and block the elongation of the DNA chain when they become incorporated. NDP kinases have been implicated in the cellular activation of nucleoside analogues, and their role needs to be clarified.

We report here a kinetic analysis of the NDP kinase reaction using a series of TDP analogues, modified at the 3′-position of deoxyribose. To compare catalytic efficiencies with normal and modified substrates, we studied the dependence of kinetic parameters on viscosity. In addition, we determined the crystal structure of *Dictyostelium* NDP kinase complexed with 3′-fluoro-2′,3′-ddUDP.

MATERIALS AND METHODS

Enzymes. Dictyostelium NDP kinase was expressed in the pJC20 expression vector, a pET derivative (*19*). It was purified by ammonium sulfate precipitation (40−80% saturation) and negative adsorption on Q-Sepharose at pH 8.5. Human NDP kinase A, expressed in the same vector, was purified by ion-exchange chromatography on Q-Sepharose (elution with a NaCl gradient from 0 to 0.5 M, at pH 7.5). Human NDP kinase B was purified by successive chromatography on Q-Sepharose and Blue Sepharose. The human NDP kinases DR-nm23 and Nm23-H4, lacking the N-terminal 17- and 33-amino acid extensions, respectively, were expressed and purified by similar methods. Details of their expression, purification, and biochemical properties will be reported elsewhere (M. Erent et al., in preparation; L. Milon et al., in preparation). *Myxococcus* NDP kinase (the PJM5C2A vector, a kind gift from R. Williams) was expressed in *Escherichia coli* and purified by ammonium sulfate precipitation and negative adsorption on Q-Sepharose.

Protein concentrations were obtained using extinction coefficients calculated from the amino acid composition (*20*), except for the *Myxococcus* and *Dictyostelium* enzymes where values of $E_{0.1\%}$ at 280 nm of 0.38 and 0.73, respectively, were obtained from amino acid analysis (kindly performed by D. Barra and A. Giartosio, University of Rome, Rome, Italy). All NDP kinases were essentially pure as ascertained by polyacrylamide gel electrophoresis in the presence of sodium dodecyl sulfate. The proteins were stored in ammonium sulfate at 90% saturation at 4 °C or in 50% glycerol at −20 °C.

Nucleotides. TDP, 3′-deoxythymidine, 2′,3′-dehydro-3′-deoxythymidine, and 3′-azido-3′-deoxythymidine were obtained from Sigma (St. Louis, MO). 3′-Fluoro-3′-deoxythymidine was synthesized by the reaction of 1-(5-*O*-trityl-2-deoxy-*β*-D-*threo*-pentofuranosyl)thymine with diethylaminosulfur trifluoride and subsequent detritylation of 5′-*O*-trityl-3′-fluoro-3′-deoxythymidine with 80% acetic acid (*21*). The ^{1}H NMR spectrum of 3′-fluoro-3′-deoxythymidine is identical to that described in the literature. All nucleosides were converted to the diphosphates by sequential phosphorylation with recombinant thymidine kinase and thymidylate kinase from *E. coli* (a gift from O. Barzu). Nucleoside phosphorylation by TK was performed at 60 °C in the presence 50 mM Tris-HCl (pH 7.4), 10 mM $MgCl_2$, and a 2-fold molar excess of ATP. To simplify the separation, ADP generated in the reaction was converted to ATP with a creatine phosphate/creatine phosphokinase regenerating system. After purification on QAE-Sephadex A25 at pH 8.0, phosphorylation to the diphosphate was performed with thymidylate kinase, in the presence of a 10% molar ratio of ATP and of the same regenerating system. The final purification was carried out on a Source Q column (1.6 cm × 12 cm), eluting with a linear gradient of LiCl at pH 4.2 (20 mM acetate buffer) at a flow rate of 2 mL/min. The nucleotides were diluted 5-fold with water, adsorbed onto the same column, and eluted with 1 M LiCl. The eluate was evaporated on a SpeedVac. LiCl was eliminated by washing with 80% ethanol. 3′-Amino-3′-dTDP was obtained by reduction of AZT-DP with a 10-fold molar excess of dithiothreitol at pH 10.5 (*22*) and purified on a Source Q column at pH 8.0. 2′,3′-Dideoxyuridine and 3′-fluoro-2′,3′-dideoxyuridine, obtained from Fluka, were phosphorylated to a mixture of di- and triphosphates in an one-pot reaction (*23*, *24*). The identities of all nucleotides, found to be pure by chromatographic analysis, were confirmed by mass spectrometry. Samples, dissolved in water/methanol/formic acid (50:50:5), were introduced into a API 365 triple-quadrupole mass spectrometer (Perkin-Elmer-Sciex, Thornill, Canada). The ionspray probe tip was held at 4.5 kV, and the orifice voltage was set at 60 V. The mass spectrometer was scanned continuously from m/z 150 to 600 with a scan step of 0.1 and a dwell time per step of 2.0 ms. Ten scans were averaged for each analysis. Mass calibration of the instrument was accomplished by matching ions of polypropylene glycol.

The nucleotide concentration was measured spectrophotometrically using the extinction coefficients of 9.6 mM^{-1} cm^{-1} at 267 nm for thymidine nucleotides and 10.0 mM^{-1} cm^{-1} at 262 nm for uridine nucleotides. Enzymatic measurements using the NDP kinase reaction in the presence of excess of ATP yielded similar concentration values (within 5%).

The pK_a of the 3′-amino group of 3′-amino-3′-dTDP was estimated by ion-exchange chromatography. A UNO-Q column (Bio-Rad) was used on a BioLogic system (Bio-Rad) with a linear 0 to 0.5 M gradient of NaCl at pH values from 6 to 9 (buffered with 50 mM MES adjusted to various pH values with Tris base). Whereas TMP and TDP exhibited nearly constant elution volumes, that of 3′-amino-3′-dTDP increased with pH, indicating that the net charge increased. A pK_a value of 8.0 was obtained by nonlinear fitting, assuming that the elution volume was a linear function of the ratio of the unprotonated and protonated forms.

Steady State Kinetic Measurements. Measurements were taken at 25 °C and pH 7.5, using a coupled assay (*1*, *25*), unless specified differently. Bovine serum albumin was included at a concentration of 1 mg/mL to stabilize enzymes. NDP kinase contamination of the pyruvate kinase from Fluka (product 83328) was negligible, but not in other pyruvate kinase preparations.

NDP kinases have a ping-pong mechanism. Their kinetic study is complicated by substrate inhibition, for nucleoside diphosphates compete with the triphosphate substrate for binding to the free enzyme, and nucleoside triphosphates compete with the diphosphate substrate for the phosphorylated enzyme, albeit with lower affinity (*26*). We therefore measured k_{cat} and k_{cat}/K_m in separate experiments, using six

to eight substrate concentrations. k_{cat} was derived by varying both ATP and NDP concentrations while keeping the [ATP]/[NTP] ratio fixed to 4.0 for TDP and 0.1−0.2 for the poorer substrates (*27*, *28*). Substrate inhibition introduces a small systematic error under these conditions (*28*), and no correction was made as the error is small compared to the variation of k_{cat} between nucleotides. k_{cat} involves the phosphorylation and dephosphorylation steps. When using a series of nucleoside diphosphates, either step can be rate-limiting, and the interpretation of k_{cat} may change. Thus, the catalytic efficiency of NDP kinases with various nucleoside diphosphates was evaluated using $(k_{cat}/K_m)_{NDP}$ as a parameter[2] to represent only the dephosphorylation step. We estimated its value for TDP by taking the ratio of the apparent k_{cat} and K_m values at a fixed concentration of 1 mM ATP. In a ping-pong mechanism, this yields the true k_{cat}/K_m. TDP analogues modified at the 3′-position have K_m values in the millimolar range. We estimated k_{cat}/K_m directly as the slope of the initial rate versus [NDP] plot, keeping the nucleoside diphosphate concentration lower than K_m by a factor of at least 5. An alternative approach for determining k_{cat}/K_m is to measure the first-order rate constant of nucleoside diphosphate consumption at a very low concentration using the coupled assay in the presence of an excess of ATP. Values obtained by this method are in good agreement with those derived from initial rate measurements. This control experiment eliminates errors due to minor nucleoside diphosphate contaminants.

Structure Determination. *Dictyostelium* NDP kinase was cocrystallized with 3′-fluoro-2′,3′-ddUDP using the hanging drop method. The drop contained 5 mg/mL protein and 15 mM nucleotide in 50 mM Tris-HCl (pH 7.5), 20 mM $MgCl_2$, and 16% PEG 6000. Crystals appeared within 2 weeks. They belong to the monoclinic space group $P2_1$ with a 100 kDa hexamer in the asymmetric unit. Diffraction data to 2.7 Å resolution were collected using a Rigaku X-ray generator with an R-axis image plate system. The data were processed with the CCP4 suite of programs (*29*). Molecular replacement performed with the nucleotide-free *Dictyostelium* NDP kinase hexamer (*7*) yielded a unique solution; an electron density map calculated from it showed density for the nucleotide bound at one of the six active sites, whereas the other sites seemed empty. Refinement with X-PLOR (*30*) was carried out without including nucleotides in the model until the *R*-factor was reduced to 30%. Given the limited resolution, noncrystallographic symmetry restraints were applied throughout refinement. At that stage, the density confirmed nearly full occupancy of the nucleotide in subunit A, and low occupancy in the other subunits; 3′-fluoro-2′,3′-ddUDP was built from TDP by removing the methyl group and replacing O3′ with fluorine, and placed in the density in subunit A. The other active sites were left empty. Further refinement reduced the *R*-factor to 20.7% with excellent geometry (Table 1). Atomic coordinates are available from the Protein Data Bank under file name 1b99.

Table 1: Statistics on Crystallographic Analysis

diffraction data	
space group	$P2_1$
asymmetric unit	hexamer
cell parameters	
a, *b*, *c* (Å)	70.0, 105.3, 70.3
α, *β*, *γ* (deg)	90, 117.4, 90
resolution (Å)	2.7
no. of unique reflections	19650
completeness (%)	81
R_{merge} (%)[a]	9.2
refinement	
R_{cryst} (%)[b]	20.7
R_{free} (%)	30.4
geometry[c]	
bond length rmsd (Å)	0.01
bond angle rmsd (deg)	1.56
torsion angle rmsd (deg)	1.25

[a] $R_{merge} = \Sigma_h|I(h)_i - \langle I(h)\rangle|/\Sigma_h I(h)_i$. [b] $R_{cryst} = \Sigma_h||F_{obs}| - |F_{calc}||/\Sigma_h|F_{obs}|$, calculated with X-PLOR on all reflections where $F > 2\sigma$. [c] Root-mean-square deviations from ideal values.

RESULTS

Steady State Kinetic Studies of Dictyostelium NDP Kinase with TDP and TDP Analogues. We used *Dictyostelium* NDP kinase for most studies since it is the NDP kinase best characterized by crystallography (*7*, *12*, *14*), physical studies (*25*, *31*), mutagenesis (*32*), and fast kinetic studies (*15*, *33*). Kinetic parameters for TDP and several analogues are given in Table 2. All compounds lacking the 3′-OH group are poor substrates, as shown by both the k_{cat} and K_m values. With 3′-dTDP, k_{cat} decreases 90-fold and K_m increases 30-fold compared to those with TDP. AZT diphosphate is an even poorer substrate. 3′-Amino-3′-dTDP is a slightly better one on a k_{cat}/K_m basis at pH 8.5. 3′-Fluoro-3′-dTDP and 2′,3′-dehydro-3′-dTDP are better substrates than 3′-dTDP and 3′-amino-3′-dTDP, in terms of both k_{cat} and k_{cat}/K_m. Very similar results were obtained with uridine nucleotides; the lack of a hydroxyl group at the 3′-position of the ribose also dramatically decreases the catalytic efficiency, and 3′-fluoro-2′,3′-ddUDP is a better substrate than 2′,3′-ddUDP.

The 3′-amino group of 3′-amino-3′-dTDP titrates with a pK_a of 8.0 (see Materials and Methods). The modified nucleotide is not a substrate, or a very poor one, in the acidic pH range where the amino group is protonated. This can be seen in a plot of k_{cat}/K_m versus pH (Figure 1). With TDP and AZT diphosphate, k_{cat}/K_m was constant between pH 6.0 and 8.0. In contrast, the NDP kinase activity on 3′-amino-3′-dTDP decreases with pH, showing that the unprotonated form of the nucleotide is the substrate and yielding a kinetic pK_a of about 8.0, consistent with the pK_a determined for the free nucleotide in solution.

Effect of Viscosity on k_{cat}/K_m. The effect of viscosity on the kinetic parameters is a useful tool for investigating the nature of the rate-limiting step in enzymatic reactions (*34*−*39*). We used this technique to check whether the rate-limiting step is the same with natural and modified substrates.

For the NDP kinase reaction shown in Scheme 1, the net rate method of Cleland (*26*) yields the following expression:

$$k_{cat}/K_m = \boldsymbol{k_4}k_5\boldsymbol{k_6}/[k_5\boldsymbol{k_6} + \boldsymbol{k_{-4}}(k_{-5} + \boldsymbol{k_6})] \qquad (2)$$

Rate constants for viscosity-sensitive steps are denoted in bold. Assuming that they are inversely proportional to the relative viscosity of the medium, we obtain the following

[2] Only $(k_{cat}/K_m)_{NDP}$ was measured in this study. The subscript has been omitted below.

Table 2: Kinetic Parameters of *Dictyostelium* NDP Kinase with Nucleoside Analogues Modified at the 3′-Position[a]

	k_{cat} (s^{-1})	K_m (mM)	k_{cat}/K_m (M^{-1} s^{-1})	$\Delta\Delta G^{\ddagger}$ (kcal/mol)[b]
TDP	1120 ± 66	0.095 ± 0.011	(11.7 ± 1.4) × 10^6	(0.0)
3′-dTDP	12.9 ± 1	3.5 ± 0.25	3600 ± 370	4.8
AZT diphosphate	5.5 ± 0.43	5.0 ± 0.75	1100 ± 140	5.5
3′-fluoro-3′-dTDP	29 ± 2.5	1.7 ± 0.2	16500 ± 1300	3.9
2′,3′-dehydro-3′-dTDP	65 ± 4	0.74 ± 0.14	56000 ± 10800	3.2
3′-amino-3′-dTDP [c]	4.0 ± 0.29	1.17 ± 0.086	5300 ± 400	4.6
2′-dUDP	875 ± 105	0.35 ± 0.08	(2.6 ± 0.28) × 10^6	(0.0)
2′,3′-ddUDP	2.3 ± 0.45	6.4 ± 1.3	360 ± 14	5.3
3′-fluoro-2′,3′-ddUDP	15.6 ± 1.48	5.5 ± 0.82	2800 ± 180	4.1

[a] k_{cat} and k_{cat}/K_m were obtained as described in Materials and Methods. [b] $\Delta\Delta G^{\ddagger} = -RT \ln[(k_{cat}/K_m)_{NDP}/(k_{cat}/K_m)_{TDP}]$ for the thymidine nucleotides, and $\Delta\Delta G^{\ddagger} = -RT \ln[(k_{cat}/K_m)_{NDP}/(k_{cat}/K_m)_{dUDP}]$ for the uridine nucleotides. The uncertainty on $\Delta\Delta G^{\ddagger}$ is ±0.25 kcal/mol, corresponding to errors of ±15% on k_{cat}/K_m. [c] Kinetic studies with 3′-amino-3′-dTDP were performed at pH 8.5 where about 76% of the amino group is unprotonated. At higher pH values, the rate of NDP kinase reaction decreased. Kinetic studies with all other nucleotides were carried out at pH 7.5.

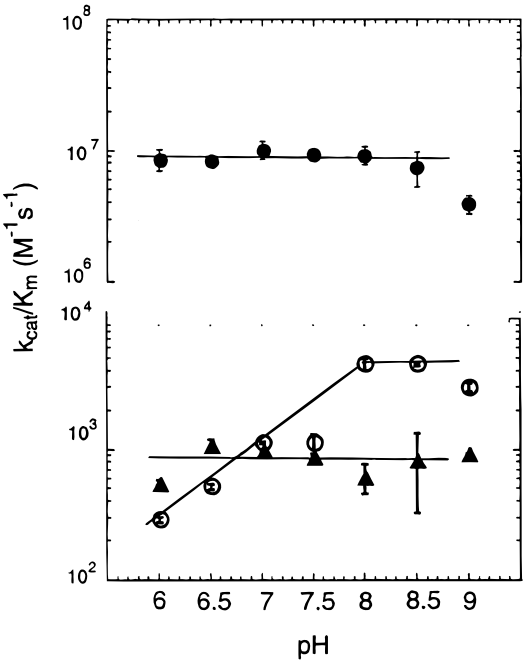

FIGURE 1: Effect of pH on the k_{cat}/K_m of the NDP kinase reaction. The donor is ATP, and acceptors are TDP (●), AZT-DP (▲), and 3′-amino-3′-dTDP (○).

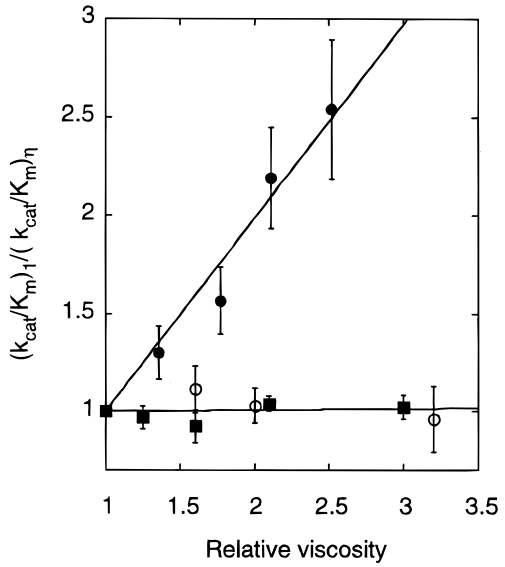

FIGURE 2: Effect of viscosity on k_{cat}/K_m. The viscogen is sucrose (black symbols) or PEG 6000 (white symbols). k_{cat}/K_m was measured for TDP (circles) and with 2′,3′-dehydro-3′-dTDP.

Scheme 1

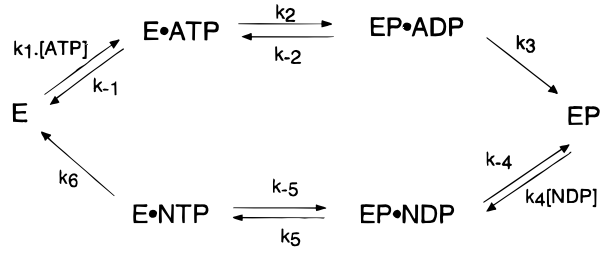

relationship for the viscosity dependence of k_{cat}/K_m for NDP:

$$(k_{cat}/K_m)_1/(k_{cat}/K_m)_\eta = [k_5\boldsymbol{k_6}\eta_{rel} + \boldsymbol{k_{-4}}(k_{-5}\eta_{rel} + \boldsymbol{k_6})]/[k_5\boldsymbol{k_6} + \boldsymbol{k_{-4}}(k_{-5} + \boldsymbol{k_6})] \quad (3)$$

where η_{rel} is the ratio of the viscosity of the medium and $(k_{cat}/K_m)_\eta$ and $(k_{cat}/K_m)_1$ are the observed k_{cat}/K_m values in the presence and in the absence of the viscogen, respectively. If the rate-limiting step is substrate diffusion, the covalent chemical steps with rate constants k_5 and k_{-5} are fast compared to substrate binding and dissociation. Thus, a plot of $(k_{cat}/K_m)_1/(k_{cat}/K_m)_\eta$ versus η_{rel} should be a straight line with a slope of 1. If on the contrary a covalent chemical step is rate-limiting, k_{cat}/K_m should not change in the presence of the viscogen.

With TDP, Figure 2 shows that k_{cat}/K_m decreases when viscosity is increased by addition of sucrose. The slope of the line is 1.0 ± 0.08, as expected if the reaction rate is fully sensitive to viscosity. In contrast to sucrose, PEG 6000, a macroviscogen, has no effect on k_{cat}/K_m. This suggests that viscogens have no nonspecific effects on protein structure. Moreover, viscosity has no effect on the rate of the NDP kinase reaction with 2′,3′-dehydro-3′-dTDP, the best modified substrate. The same absence of an effect was found with AZT-DP and 3′-amino-3′-dTDP (not shown in Figure 2 for clarity). It suggests that the rate-limiting step is different with TDP and with the modified substrates. With the natural substrate, the covalent steps are fast and the overall reaction may be diffusion-limited, although the k_{cat}/K_m value is lower than the second-order rate constant predicted for a diffusion-controlled reaction.[3] With the modified substrates, the covalent step becomes much slower and rate-limiting. The

[3] This has been found with other enzymes and is discussed in ref *37*.

Table 3: Effect of Ribose Modification on k_{cat}/K_m with Different NDP Kinases[a]

	HA	HB	DR	H4	Dd	Myxo
TDP	$(2.6 \pm 0.17) \times 10^6$	$(2 \pm 0.14) \times 10^6$	$(0.9 \pm 0.2) \times 10^6$	$(2.4 \pm 0.17) \times 10^6$	$(11.7 \pm 1.4) \times 10^6$	$(4.4 \pm 0.43) \times 10^6$
3′-dTDP	85 ± 12	72 ± 10	25 ± 1.1	135 ± 21	3600 ± 370	436 ± 32
$\Delta\Delta G^‡$ (kcal/mol)	6.2	6.1	6.3	5.8	4.8	5.5
AZT diphosphate	152 ± 13	174 ± 9	34 ± 4.5	215 ± 18	1100 ± 140	135 ± 20
$\Delta\Delta G^‡$ (kcal/mol)	5.8	5.6	6.1	5.5	5.5	6.2
3′-fluoro-3′-dTDP	849 ± 27	565 ± 38	259 ± 10	645 ± 85	16500 ± 1300	7760 ± 504
$\Delta\Delta G^‡$ (kcal/mol)	4.8	4.9	4.9	4.9	3.9	3.8
2′,3′-dehydro-3′-dTDP	862 ± 99	519 ± 26	302 ± 15	952 ± 124	56000 ± 10800	10700 ± 1400
$\Delta\Delta G^‡$ (kcal/mol)	4.8	4.9	4.8	4.7	3.2	3.6

[a] HA, human NDP kinase A; HB, human NDP kinase B; DR, human DR-nm23; H4, human Nm23-H4; Dd, *Dictyostelium* NDP kinase; Myxo, *Myxococcus* NDP kinase. k_{cat}/K_m values are expressed in M^{-1} s^{-1}. $\Delta\Delta G^‡$ values were calculated as described in the footnote of Table 2.

absence of the 3′-OH group therefore has a larger effect on the transition state of the chemical step than the $\Delta\Delta G^‡$ values reported in Tables 2 and 3.

Steady State Kinetic Analysis with Several NDP Kinases. The active site of NDP kinases is remarkably conserved during evolution, as ascertained by crystal structures and sequence alignment. All residues making polar contacts and hydrogen bonds with nucleotide substrates are identical in all known NDP kinases. Variability nevertheless appears at the level of the quaternary structure (some NDP kinases are tetrameric, and others are hexameric), and of physical parameters such as the thermal stability. To detect possible effects of structural modifications on substrate selectivity, we measured k_{cat}/K_m for TDP and its analogues with several NDP kinases (Table 3). In all cases, catalysis was severely impaired in the absence of a 3′-hydroxyl group on the substrate. Human NDP kinases appear to be more selective than the enzymes from lower organisms. Whereas *Dictyostelium* enzyme is slightly more efficient with 3′-dTDP than with AZT-DP, the converse is true for other NDP kinases. The similarity of the kinetic parameters observed for the four human NDP kinases is remarkable given that, while NDP kinases A and B are 88% identical in sequence, the identity level is only ≈65% with DR-Nm23, and 55% with Nm23-H4 (*40*−*42*). These differences in sequence do not appear to affect the catalytic site.

Structure of the Complex of Dictyostelium NDP Kinase with 3′-Fluoro-2′,3′-ddUDP. 3′-Fluoro-2′,3′-ddUDP and 3′-fluoro-3′-dTDP are poor substrates for *Dictyostelium* NDP kinase, but they are still better than the dideoxy analogues 3′-dTDP and 2′,3′-ddUDP (Table 2). To elucidate the role of the fluorine substituent, we determined the X-ray structure of the complex with 3′-fluoro-2′,3′-ddUDP to 2.7 Å resolution. In the crystal, the modified nucleotide was found to be distributed unequally among the six subunits of the hexamer. In subunit A, the electron density is unequivocal (Figure 3A). In the other subunits, the density is low, indicating occupancies of less than 30%, and the sites were considered empty. Unequal occupancy of otherwise equivalent sites was observed in other NDP kinase X-ray structures [e.g., in the complex with ADP (*10*)] and may be an artifact caused by crystal packing. The subunit containing 3′-fluoro-2′,3′-ddUDP has a conformation similar to the one observed in complexes with ADP and with TDP (*10*, *12*). It differs from the conformation of the free protein by a 2 Å movement of a pair of surface helices (helices αA and α2), closing on the base moiety the cleft where the nucleotide binds. However, the movement is smaller with 3′-fluoro-2′,3′-ddUDP than with TDP, and the cleft is more open. The tertiary structure is otherwise the same as that in the TDP complex, and the root-mean-square displacement of the main chain atoms is only 0.4 Å.

In Figure 3B, we illustrate the conformation of the bound 3′-fluoro-2′,3′-ddUDP and compare it to that of bound TDP. The two differ by a shift of the plane of the base and by the puckering of the sugar, which is C3′-endo for TDP and C2′-endo for the analogue (Table 5). As a consequence of the puckering, the fluorine does not exactly replace the 3′-OH of TDP, but is located 1.3 Å away. The C2′-endo puckering mode is also observed with AZT diphosphate bound to NDP kinase (*13*). A magnesium ion probably ligates the two phosphates of 3′-fluoro-2′,3′-ddUDP as it does for TDP, but the electron density is weak. 3′-Fluoro-2′,3′-ddUDP and TDP form the same interactions with protein groups, with one important exception. In TDP and in other natural nucleotide substrates of NDP kinase, the 3′-OH group accepts two hydrogen bonds from the amido nitrogen of Asn119 and the amino group of Lys16, and donates one to O7 of the β-phosphate (Figure 3C). The fluorine atom of 3′-fluoro-2′,3′-ddUDP is a potential hydrogen bond acceptor, but not a donor, and its position is different from that of the 3′-OH. In the complex, the hydrogen bond with Lys16 is maintained and another may be formed with the hydroxyl of Tyr56, but the bonds with Asn119 and the β-phosphate cannot be made. Instead, these two groups hydrogen bond to each other, which is made possible by a shift of the β-phosphate. This group moves away from His122 (Figure 3B), and the distance between O7 and Nδ of His122 increases from 4.9 to 5.3 Å.

DISCUSSION

Structure−*Activity Relationships.* Our results emphasize the role of the ribose 3′-hydroxyl group in catalysis. In all structures of nucleotides bound to NDP kinases (*9*−*13*), the nucleotide 3′-OH group donates a hydrogen bond to O7, the oxygen atom which bridges the β- and γ-phosphates in a nucleoside triphosphate. This bond has also been seen in the structure of NDP kinase complexed with ADP and AlF_3, a model for the transition state (*14*). The absence of a 3′-OH group in the modified nucleotides has a large effect on the kinetic parameters, decreasing k_{cat} and increasing K_m. With *Dictyostelium*, but not with human NDP kinases, the catalytic efficiency is further reduced for AZT diphosphate. The structure of this modified nucleotide in complex with a point mutant of *Dictyostelium* NDP kinase exhibits significant changes with respect to TDP in the sugar conformation and

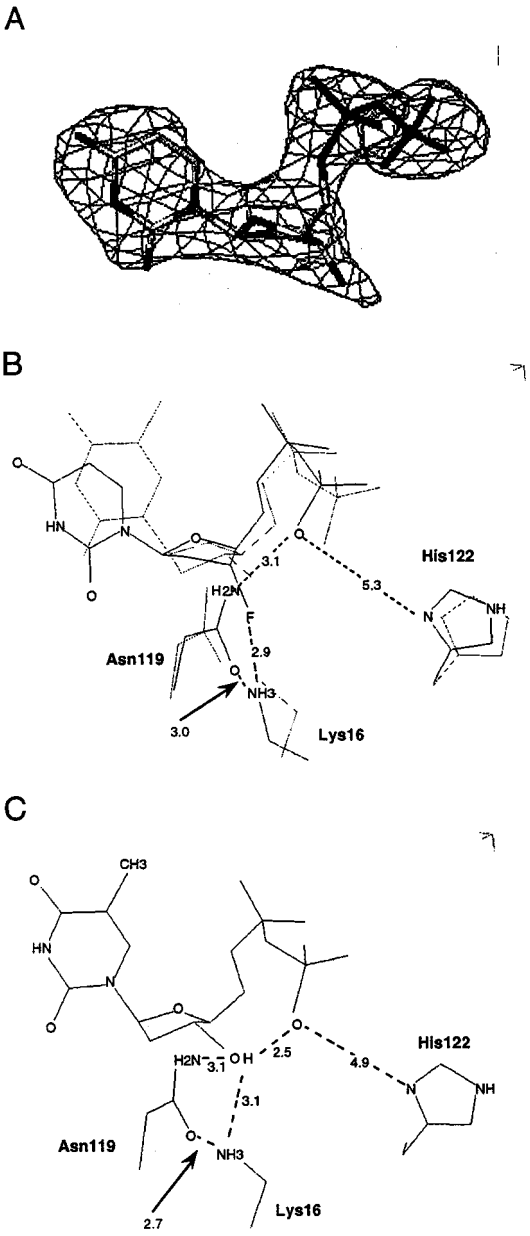

FIGURE 3: Structure of 3′-fluoro-2′,3′-ddUDP complexed with the *Dictyostelium* NDP kinase. (A) Model of the modified nucleotide in its electron density. The difference map is contoured at 2.5σ. (B) Relevant nucleotide interactions with active-site side chains (see also Table 4). The thin line is TDP in the complex with the enzyme (*12*). The Cα atoms of the two structures were aligned using the SwissPDBViewer software. The interactions of TDP with the protein are shown in panel C. Distances are in angstroms.

the position of helices αA and α2 which close the active site (*13*).

3′-Fluoro-3′-dTDP is a better substrate than 3′-dTDP, and the same applies to uridine nucleotides (Table 2). Compared to enzyme-bound TDP, the structure of the complex with NDP kinase exhibits important differences for the fluorinated analogue. The hydrogen bond between the 3′-hydroxyl group and the β-phosphate is replaced by a longer bond between the β-phosphate and Asn119 (Figure 3B,C). The β-phosphate is farther away from His122 and the sugar puckering C2′-endo instead of C3′-endo. The sugar conformation of the bound nucleotide seems to be a crucial factor. Natural substrates are C3′-endo in complexes with ADP, TDP, GDP, and ADP−AlF_3; poor substrates are C2′-endo in complexes

Table 4: Nucleotide Contacts[a]

protein		3′-fluoro-3′-deoxyTDP	TDP[b]
base	Phe64 ring	3.6	3.6
	Val116	3.7	3.6
ribose			
X3′[c]	Nξ Lys16	2.8	3.1
	Nδ2 Asn119		3.1
	Oϵ Tyr56	2.9	
α-phosphate			
O11	Nϵ2 His59		3.5
	Mg^{2+}		2.1
O12	Oγ Thr98		3.4
β-phosphate			
O11	Nη1 Arg95	3.1	2.9
	Mg^{2+}	2.8[d]	2.1
O22	Nη1 Arg92		2.9
	Oγ Thr98	3.3	3.3
	Nη2 Arg109		2.8
O7	Nη1 Arg109	3.0	3.0
	Nδ2 Asn119	2.9	

[a] Distances in angstroms. [b] Values from ref *12*. [c] X is fluorine in 3′-fluoro-3′-deoxyTDP and oxygen in TDP. [d] Due to poor density, Mg^{2+} was modeled as a water molecule.

Table 5: Conformation of the Bound Nucleotide[a]

nucleotide	3′-fluoro-2′,3′-ddUDP	AZT diphosphate[b]	TDP[c]
glycosyl bond χ (deg)	−124	−127	−156
C4′−C5′ γ (deg)	67	59	57
pucker mode	C2′-endo	C2′-endo	C3′-endo
angle *p* (deg)	114	158	31

[a] Dihedral angles χ (O4′−C1′−N1−C2) and γ (O5′−C5′−C4′−C3′), phase angle *p*, and the pucker mode are defined in ref *62*. [b] From ref *13*. Crystals of the AZT diphosphate complex contain three subunits per asymmetric unit, and the values are for subunit B. [c] From ref *12*.

with 3′-fluoro-2′,3′-ddUDP and AZT diphosphate. In addition, the bulky azido group of AZT diphosphate cannot be accommodated into the binding site in the TDP conformation. Nevertheless, 3′-dTDP and AZT diphosphate have similar substrate efficiencies and sugar puckering. This suggests that NDP kinases have a second binding mode for their substrates in the absence of a 3′-hydroxyl group.

3′-Amino-3′-dTDP is a poor substrate in the unprotonated state, and barely a substrate at all when it is protonated. Presumably, the protonated 3′-amino group does not allow binding near Lys16, which is also positively charged, due to electrostatic repulsion. In principle, the amino group could be a good analogue of the OH group, but our kinetic (Table 2) and structural data (Y. Xu et al., unpublished results) indicate that it is not.

Surprisingly, 2′,3′-dehydro-3′-dTDP is the best substrate among the TDP analogues modified at the 3′-position that we tested. This can be explained as follows. In 2′,3′-dehydro-3′-dTDP, the planar structure of the double bond may leave room for a water molecule to bind near the position of the missing hydroxyl oxygen. In 3′-dTDP, the different geometry and nonpolar character of the C2′ methylene may be less favorable for binding water. The water molecule could then make hydrogen bonds with the β-phosphate, Lys16, and Asn119. In a similar way, a water molecule was found to replace the missing 2′-OH group in the NDP kinase−TDP complex (*12*).

How Does the 3′-Hydroxyl Group Assist Catalysis? The structure of NDP kinase complexed with ADP and AlF_3 is

a good approximation of the transition state during phosphoryl transfer. Yet, a comparison of this structure with that of NDP kinase complexed with ADP or TDP, which is a model of the ground state, offers no immediate explanation of the rate acceleration, for no new interaction is apparent with the transition state. The hydrogen bond connecting the 3′-OH to O7 in the β-phosphate is present in all crystal structures of NDP kinase−nucleotide complexes, though it may be somewhat shorter in the transition state analogue. The distance between O7 and the acceptor Nδ atom of His122 is 4.8 Å in the NDP kinase−ADP−AlF_3 structure (*14*), much longer than the sum of covalent bonds (3.4 Å) but shorter that the sum of the van der Waals radii (*43*). There is no reason to believe that the 3′-OH−O7 bond is a low-barrier hydrogen bond (*44*), for the pK_a values of the two oxygen atoms are far apart (pK_a of <7 for O7 in ADP and ∼14 for the 3′-OH). In ATP, O7 is the oxygen atom bridging the β- and γ-phosphates. If the phosphate transfer mechanism has a substantial dissociative character, the charge on O7 should increase during histidine phosphorylation (reaction 1a), making the hydrogen bond stronger in the transition state (*43*, *45*−*47*). The principle of microscopic reversibility states that the transition state is the same for dephosphorylation (reaction 1b). On the other hand, the 3′-OH−O7 hydrogen bond keeps the nucleotide in the particular conformation that gives the best fit of the transition state to the active site. Interactions made by the oxygen atom bridging the β- and γ-phosphates of GTP in the transition state have been recently shown to be crucial for the GTPase activity of $p21^{ras}$ (*47*, *48*).

The participation of groups carried by the substrate in enzymatic catalysis is not unusual in phosphate transfer. The 2′-hydroxyl of ribose is known to participate as a nucleophile in the reaction catalyzed by pancreatic ribonuclease, and Herschlag et al. (*49*) demonstrated that it also participates in the reaction catalyzed by the *Tetrahymena* ribozyme. In the ribozyme as in NDP kinase, fluorine at the 2′-position of the nucleotide had a favorable effect with respect to the deoxynucleotide, although it cannot donate a hydrogen bond as the hydroxyl group does, and rate acceleration by an inductive effect was suggested.

The participation of substrate groups in catalysis has been suggested in a few other cases. In the restriction enzyme *Eco*RV, one of the phosphoryl oxygen atoms of the DNA substrate activates the attacking water molecule (*50*). Cases of mutant enzymes where a missing active group could be replaced by part of the substrate have also been reported (*51*−*54*). Substrate-assisted catalysis is believed to be an intermediate step during the evolution from the RNA world to the protein world (*52*). In this respect, NDP kinase is a surprising example where nature did not manage to replace the ribose 3′-hydroxyl with a protein side chain.

Relevance for Antiviral Therapy. Most nucleoside analogues used as antiviral drugs are modified at the 3′-position of the ribose (*55*). After phosphorylation to triphosphate by cellular enzymes, these compounds are incorporated into the DNA, preventing further chain elongation. Thus, 3′-deoxythymidine, 2′,3′-dehydro-3′-deoxythymidine (D4T), and 3′-azido-3′-deoxythymidine (AZT) are anti-AIDS drugs; 3′-fluoro-3′-deoxythymidine also displays anti-AIDS activity, but it is more toxic than AZT (*18*). A knowledge of the substrate specificity of the candidate enzymes involved in cellular phosphorylation of nucleoside analogues is therefore of primary medicinal importance. Phosphorylation of AZT to the monophosphate is not rate-limiting in vivo, since in cell cultures and in human peripheral blood mononuclear cells of patients, the drug accumulates mostly in the monophosphate form, which is toxic at high concentrations (*56*−*59*). AZT monophosphate is a poor substrate for thymidylate kinase, and that step is a bottleneck of AZT activation (*60*). NDP kinase is a second bottleneck. AZT is found in treated cells as diphosphate and triphosphate in similar amounts (*61*). With good substrates of NDP kinase, the phosphorylation reaction is at equilibrium and the [NDP]/[NTP] ratio equal to the [ADP]/[ATP] ratio, which is much ≪1. Analogues which are better substrates for NDP kinase in vitro are also better converted to the triphosphate in vivo. A dramatic effect may be seen in vivo even if the in vitro effect is rather small. Thus, the triphosphate forms of 3′-fluoro-3′-deoxythymidine and 2′,3′-dehydro-3′-deoxythymidine occur at much higher concentrations than for AZT, and their mono- and diphosphate concentrations are much lower (*61*). This fits with the results of our kinetic and structural studies of NDP kinase and should encourage a thorough analysis of the enzymatic properties of other cellular kinases with nucleotide analogues as substrates.

ACKNOWLEDGMENT

We are grateful to Drs. Angela De Otero and Jacqueline Cherfils for carefully reading the manuscript and helpful comments, Octavian Barzu, Roger Williams, and Manfred Konrad for enzymes and plasmids, Donatella Barra and Anna Giartosio for the determination of the extinction coefficients by amino acid analysis, Abdelkader Namane for mass spectrometry, and Dr. Jean-Yves Daniel for discussion.

REFERENCES

1. Parks, R. E., Jr., and Agarwal, R. P. (1973) *The Enzymes (3rd Ed.) 8*, 307−334.
2. Frey, P. A. (1992) *Enzymes (3rd Ed.) 20*, 142−186.
3. Lecroisey, A., Lascu, I., Bominaar, A., Veron, M., and Delepierre, M. (1995) *Biochemistry 34*, 12445−12450.
4. Morera, S., Chiadmi, M., LeBras, G., Lascu, I., and Janin, J. (1995) *Biochemistry 34*, 11062−11070.
5. Lascu, I., Morera, S., Chiadmi, M., Cherfils, J., Janin, J., and Veron, M. (1996) in *Techniques in Protein Chemistry* (Marshak, D. R., Ed.) Vol. VII, pp 209−217, Academic Press, San Diego, CA.
6. Dumas, C., Lascu, I., Morera, S., Glaser, P., Fourme, R., Wallet, V., Lacombe, M.-L., Veron, M., and Janin, J. (1992) *EMBO J. 11*, 3203−3208.
7. Morera, S., LeBras, G., Lascu, I., Lacombe, M. L., Veron, M., and Janin, J. (1994) *J. Mol. Biol. 243*, 873−890.
8. Chiadmi, M., Lascu, I., Veron, M., and Janin, J. (1993) *Structure 1*, 283−293.
9. Williams, R. L., Oren, D. A., Munoz-Dorado, J., Inouye, S., Inouye, M., and Arnold, E. (1993) *J. Mol. Biol. 234*, 1230−1247.
10. Morera, S., Lascu, I., Dumas, C., LeBras, G., Briozzo, P., Veron, M., and Janin, J. (1994) *Biochemistry 33*, 459−467.
11. Morera, S., Lacombe, M. L., Xu, Y., LeBras, G., and Janin, J. (1995) *Structure 3*, 1307−1314.
12. Cherfils, J., Morera, S., Lascu, I., Veron, M., and Janin, J. (1994) *Biochemistry 33*, 9062−9069.
13. Xu, Y., Sellam, O., Morera, S., Sarfati, S., Biondi, R., Veron, M., and Janin, J. (1997) *Proc. Natl. Acad. Sci. U.S.A. 94*, 7162−7165.

14. Xu, Y., Morera, S., Janin, J., and Cherfils, J. (1997) *Proc. Natl. Acad. Sci. U.S.A. 94*, 3579−3583.
15. Schneider, B., Xu, Y. W., Sellam, O., Sarfati, R., Janin, J., Veron, M., and Deville-Bonne, D. (1998) *J. Biol. Chem. 273*, 11491−11497.
16. Bourdais, J., Biondi, R., Sarfati, S., Guerreiro, C., Lascu, I., Janin, J., and Veron, M. (1996) *J. Biol. Chem. 271*, 7887−7890.
17. Kuby, S. A., Fleming, G., Alber, T., Richardson, D., Takeneka, H., and Hamada, M. (1991) *Enzyme 45*, 1−13.
18. De Clercq, E. (1992) *AIDS Res. Hum. Retroviruses 8*, 119−134.
19. Clos, J., Westwood, J. T., Becker, P. G., Wilson, S., Lambert, K., and Wu, C. (1990) *Cell 63*, 1085−1097.
20. Gill, S. G., and von Hippel, P. H. (1989) *Anal. Biochem. 182*, 319−326.
21. Herdewijn, P., Balzarini, J., De Clercq, E., Pauwels, R., Baba, M., Broder, S., and Vanderhaeghe, H. (1987) *J. Med. Chem. 30*, 1270−1278.
22. Reardon, J. E., Crouch, R. C., and St John-Williams, L. (1994) *J. Biol. Chem. 269*, 15999−16008.
23. Hoffmann, C., Genieser, H.-G., Veron, M., and Jastorff, B. (1996) *Biol. Org. Chem. Lett. 6*, 2571−2574.
24. Yoshikawa, M., Kato, T., and Takenishi, T. (1969) *Bull. Chem. Soc. Jpn. 42*, 3505−3508.
25. Lascu, I., Deville-Bonne, D., Glazer, P., and Véron, M. (1993) *J. Biol. Chem. 268*, 20268−20275.
26. Cleland, W. W. (1977) *Adv. Enzymol. 45*, 273−387.
27. Segel, I. H. (1993) *Enzyme kinetics*, Wiley, New York.
28. Garces, E., and Cleland, W. W. (1969) *Biochemistry 8*, 633−640.
29. Collaborative Computational Project, Number 4 (1994) *Acta Crystallogr., Sect. D 50*, 760−763.
30. Brünger, A. T., Kuriyan, J., and Karplus, M. (1987) *Science 235*, 458−460.
31. Mesnildrey, S., Agou, F., Karlsson, A., Deville-Bonne, D., and Veron, M. (1998) *J. Biol. Chem. 273*, 4436−4442.
32. Tepper, A. D., Dammann, H., Bominaar, A. A., and Veron, M. (1994) *J. Biol. Chem. 269*, 32175−32180.
33. Deville-Bonne, D., Sellam, O., Merola, F., Lascu, I., Desmadril, M., and Veron, M. (1996) *Biochemistry 35*, 14643−14650.
34. Tian, G. T., Yan, H., Jiang, R.-T., Kishi, F., Nakazawa, A., and Tsai, M.-D. (1990) *Biochemistry 29*, 4296−4304.
35. Blacklow, S. C., Raines, R. T., Lim, W. A., Zamore, P. D., and Knowles, J. R. (1988) *Biochemistry 27*, 1158−1167.
36. Adams, J. A., and Taylor, S. S. (1992) *Biochemistry 31*, 8516−8522.
37. Caldwell, S. R., Newcomb, J. R., Schlecht, K. A., and Raushel, F. M. (1991) *Biochemistry 30*, 7438−7444.
38. Glickman, M. H., and Klinnman, J. P. (1995) *Biochemistry 34*, 14077−14092.
39. Cleland, W. W. (1990) *The Enzymes (3rd Ed.) 19*, 99−158.
40. Gilles, A. M., Presecan, E., Vonica, A., and Lascu, I. (1991) *J. Biol. Chem. 266*, 8784−8789.
41. Venturelli, D., Martinez, R., Melotti, P., Casella, I., Peschle, C., Cucco, C., Spampinato, G., Darzynkiewicz, Z., and Calabretta, B. (1995) *Proc. Natl. Acad. Sci. U.S.A. 92*, 7435−7439.
42. Milon, L., Rousseau-Merck, M.-F., Munier, A., Erent, M., Lascu, I., Capeau, J., and Lacombe, M.-L. (1996) *Hum. Genet. 99*, 550−557.
43. Schlichting, I., and Reinstein, J. (1997) *Biochemistry 36*, 9290−9296.
44. Cleland, W. W., Frey, P. A., and Gerlt, J. A. (1998) *J. Biol. Chem. 273*, 25529−25532.
45. Matte, A., Tavi, L. W., and Delbaere, T. J. (1998) *Structure 6*, 413−419.
46. Mildvan, A. S. (1997) *Proteins: Struct., Funct., Genet. 29*, 401−416.
47. Admiraal, S. J., and Herschlag, D. (1995) *Chem. Biol. 2*, 729−739.
48. Cepus, B., Scheidig, A. J., Goody, R. S., and Gerwart, K. (1998) *Biochemistry 37*, 10263−10271.
49. Herschlag, D., Eckstein, F., and Cech, T. R. (1993) *Biochemistry 32*, 8312−8321.
50. Jeltsch, A., Alves, J., Wolfes, H., Maass, G., and Pingoud, A. (1993) *Proc. Natl. Acad. Sci. U.S.A. 90*, 8499−8503.
51. Corey, D. R., Willett, W. S., Coombs, G. S., and Craik, C. S. (1995) *Biochemistry 34*, 11521−11527.
52. Carter, P., and Wells, J. A. (1987) *Science 237*, 394−399.
53. Carter, P., Abrahmsen, L., and Wells, J. A. (1991) *Biochemistry 30*, 6142−6148.
54. Zor, T., Bar-Yaacov, M., Elgavish, S., Shaanan, B., and Selinger, Z. (1997) *Eur. J. Biochem. 249*, 330−336.
55. Balzarini, J. (1994) *Pharm. World Sci. 16*, 113−126.
56. Tornevik, Y., Jacobsson, B., Britton, S., and Eriksson, S. (1991) *AIDS Res. Hum. Retroviruses 7*, 751−759.
57. Slusher, J. T., Kuwahara, S. K., Hamzeh, F. M., Lewis, L. D., Kornhauser, D. M., and Lietman, P. S. (1992) *Antimicrob. Agents Chemother. 36*, 2473−2477.
58. Tornevik, Y., Ullman, B., Balzarini, J., Wahren, B., and Eriksson, S. (1995) *Biochem. Pharmacol. 49*, 829−837.
59. Balzarini, J., Baba, M., Pauwels, R., Herdewijn, P., and De Clercq, E. (1988) *Biochem. Pharmacol. 37*, 2847−2856.
60. Lavie, A., Schlichting, I., Vetter, I. R., Konrad, M., Reinstein, J., and Goody, R. S. (1997) *Nat. Med. 3*, 922−924.
61. Balzarini, J., Herdewijn, P., and De Clercq, E. (1989) *J. Biol. Chem. 264*, 6127−6133.
62. Saenger, W. (1984) *Principles of Nucleic Acid Structure*, Springer, New York.

BI982990V